Mechanism of Enantioselective Ti-Catalyzed Strecker Reaction: Peptide-Based Metal Complexes as Bifunctional Catalysts

Nathan S. Josephsohn, Kevin W. Kuntz, Marc L. Snapper,* and Amir H. Hoveyda*

Contribution from the Department of Chemistry, Merkert Chemistry Center, Boston College, Chestnut Hill, Massachusetts 02467

Received August 2, 2001

Abstract: Kinetic, structural, and stereochemical data regarding the mechanism of Ti-catalyzed addition of cyanide to imines in the presence of Schiff base peptide ligands are disclosed. The reaction is first order in the Ti·ligand complex; kinetic studies reveal $\Delta S^{\ddagger} = -45.6 \pm 4.1$ cal K^{-1} mol^{-1}, indicating a highly organized transition structure for the turnover-limiting step of the catalytic cycle. A mechanistic model consistent with the kinetic and stereochemical data is presented, where the Ti center is coordinated to the Schiff base unit of the ligand and the AA2 moiety of the peptidic segment of the chiral ligand associates and *delivers* HNC to the activated bound substrate. Thus, these studies illustrate that these non-C_2-symmetric catalysts likely operate in a bifunctional fashion.

Introduction

From the standpoint of catalytic asymmetric reaction development, peptidic Schiff bases represented by **I**−**III** (Chart 1) are attractive for several reasons: (i) their structural modularity allows for facile preparation of catalyst libraries,[1](ii) their non-C_2-symmetric structure[2] readily lends itself to diversification, and (iii) the availability of multiple Lewis acid binding sites raises the possibility of multifunctional catalysis.[3] These chiral dipeptides have thus emerged as highly versatile ligands for enantioselective catalysis: Ligands **I** effect an assortment of asymmetric transformations that include Ti-catalyzed addition of cyanide to aldehydes,[4] epoxides,[5] and imines,[6] Al-catalyzed addition of cyanide to ketones,[7] and Zr-catalyzed addition of dialkylzincs to imines.[8] Moreover, dipeptides **II** and **III** have been employed to promote facile and enantioselective Cu-catalyzed conjugate additions[9] and allylic substitutions[10] with alkylzincs. Such advances and the related high levels of reactivity and enantioselectivity render mechanistic information regarding the inner workings of this class of chiral catalysts valuable, especially in connection with future efforts aimed toward the development of new catalytic asymmetric processes.

Chart 1

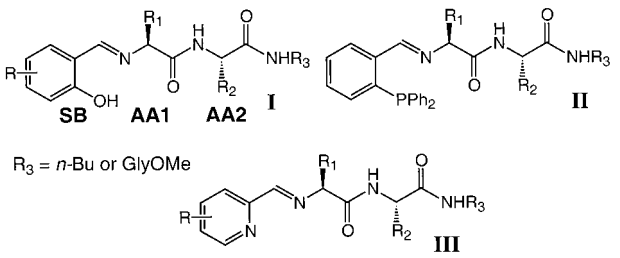

Herein, we disclose kinetic and structural data that, for the first time, shed light on one of the key transformations promoted by this versatile class of chiral ligands. The Ti-catalyzed addition of cyanide to imines[6] is a C−C bond forming process that is promoted by ligands **I** and affords nonracemic amino nitriles (e.g., **3**, Scheme 1) which may then be converted to optically pure α-amino acids (e.g., **4**, Scheme 1).[11] The results presented below show that in effecting the Ti-catalyzed addition, *these non-C_2 symmetric catalysts likely operate in a bifunctional*

(1) Shimizu, K. D.; Snapper, M. L.; Hoveyda, A. H. *Chem.*−*Eur. J.* **1998**, *4*, 1885−1889.

(2) Pfaltz, A. In *Stimulating Topics in Organic Chemistry*; Shibasaki, M., Stoddard, J. F., Vogtle, F., Eds.; VCH-Wiley: Weinheim, 2000, pp 89−103.

(3) (a) Steinhagen, H.; Helmchen, G. *Angew. Chem., Int. Ed. Engl.* **1996**, *35*, 2339−2342. (b) Shibasaki, M.; Sasai, H.; Arai, T. *Angew. Chem., Int. Ed. Engl.* **1997**, *36*, 1236−1256. (c) Rowlands, G. J. *Tetrahedron* **2001**, *57*, 1865−1882.

(4) Mori, A.; Abe, H.; Inoue, S. *Appl. Organomet. Chem.* **1995**, *9*, 189−197 and references therein.

(5) (a) Cole, B. M.; Shimizu, K. D.; Krueger, C. A.; Harrity, J. P.; Snapper, M. L.; Hoveyda, A. H. *Angew. Chem., Int. Ed. Engl.* **1996**, *35*, 1668−1671. (b) Shimizu, K. D.; Cole, B. M.; Krueger, C. A.; Kuntz, K. W.; Snapper, M. L.; Hoveyda, A. H. *Angew. Chem., Int. Ed. Engl.* **1997**, *36*, 1704−1707.

(6) (a) Krueger, C. A.; Kuntz, K. W.; Dzierba, C. D.; Wirschun, W. G.; Gleason, J. D.; Snapper, M. L.; Hoveyda, A. H. *J. Am. Chem. Soc.* **1999**, *121*, 4284−4285. (b) Porter, J. R.; Wirschun, W. G.; Kuntz, K. W.; Snapper, M. L.; Hoveyda, A. H. *J. Am. Chem. Soc.* **2000**, *122*, 2657−2658. (c) For a review on catalytic asymmetric additions to imines, see: Kobayashi, S.; Ishitani, H. *Chem. Rev.* **1999**, *99*, 1069−1094. (d) Enders, D.; Reinhold, U. *Tetrahedron: Asymmetry* **1997**, *8*, 1895−1946.

(7) Deng, H.; Isler, M. P.; Snapper, M. L.; Hoveyda, A. H. Manuscript in preparation.

(8) (a) Porter, J. R.; Traverse, J. F.; Hoveyda, A. H.; Snapper, M. L. *J. Am. Chem. Soc.* **2001**, *123*, 984−985. (b) Porter, J. R.; Traverse, J. F.; Hoveyda, A. H.; Snapper, M. L. *J. Am. Chem. Soc.* **2001**, *123*, 10409−10410.

(9) Degrado, S. J.; Mizutani, H.; Hoveyda, A. H. *J. Am. Chem. Soc.* **2001**, *123*, 755−756.

(10) Luchaco-Cullis, C. A.; Mizutani, H.; Murphy, K. E.; Hoveyda, A. H. *Angew. Chem., Int. Ed. Engl.* **2001**, *40*, 1456−1460.

(11) For related studies on catalytic asymmetric cyanide addition to imines, see: (a) Iyer, M. S.; Gigstad, K. M.; Namdev, N. D.; Lipton, M. *J. Am. Chem. Soc.* **1996**, *118*, 4910−4911. (b) Sigman, M. S.; Jacobsen, E. N. *J. Am. Chem. Soc.* **1998**, *120*, 4901−4902. (c) Sigman, M. S.; Jacobsen, E. N. *J. Am. Chem. Soc.* **1998**, *120*, 5315−5316. (d) Ishitani, H.; Komiyama, S.; Kobayashi, S. *Angew. Chem., Int. Ed. Engl.* **1998**, *37*, 3186−3188. (e) Corey, E. J.; Grogan, M. *Org. Lett.* **1999**, *1*, 157−160. (f) Ishitani, H.; Komiyama, S.; Hasegawa, Y.; Kobayashi, S. *J. Am. Chem. Soc.* **2000**, *122*, 762−766. (g) Takamura, M.; Hamashima, Y.; Usuda, H.; Kanai, M.; Shibasaki, M. *Angew. Chem., Int. Ed. Engl.* **2000**, *39*, 1650−1652. (h) Sigman, M. S.; Vachal, P.; Jacobsen, E. N. *Angew. Chem., Int. Ed. Engl.* **2000**, *39*, 1279−1281. (i) Nogami, H.; Matsunaga, S.; Kanai, M.; Shibasaki, M. *Tetrahedron Lett.* **2001**, *42*, 279−283.

10.1021/ja011875w CCC: $20.00
Published on Web 11/01/2001

Scheme 1

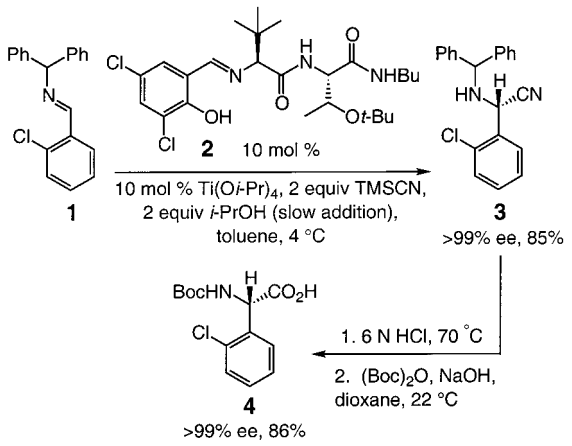

manner. The Ti·Schiff base (SB) coordinates with the substrate, while an amide moiety within the peptide segment associates and delivers cyanide to the activated imine. Experimental evidence and subsequent modeling studies indicate that proper disposition of different Lewis basic sites within the ligand structure allow the SB and amide carbonyls in AA1 and AA2 to provide complementary functions, giving rise to high yields and enantioselectivities.

Results and Discussion

A key observation regarding the Ti-catalyzed process is that slow addition of an alcohol (e.g., *i*-PrOH) to the reaction mixture is required to achieve appreciable levels of conversion (>98%).[6a,b] We thus reasoned that HCN (or HNC), not TMSCN, may be participating in the transformation. That is, slow generation of HCN, from reaction of the alcohol additive and TMSCN, might ensure minimal levels of uncatalyzed and nonselective C−C bond formation (HCN can add to imines in the absence of a catalyst). We subsequently established that slow addition of cyanide (without added *i*-PrOH, under identical conditions) does indeed lead to similar levels of reactivity and asymmetric induction[6a] as observed with TMSCN in the presence of *i*-PrOH.[12]

Because a number of Ti-catalyzed reactions have been shown to proceed through pathways involving dimeric or oligomeric complexes,[5b,13] we determined that there is a linear correlation between catalyst and product ee (Figure 1).[14] Subsequent kinetic studies ($k_{obs} = 5.35 \pm 0.50 \times 10^{-5}$ s^{-1} at 22 °C) indicate that the reaction is first order in the catalyst ($R^2 = 0.9973$). The necessary data were obtained by monitoring reaction progress (disappearance of substrate C═N absorption) with a ReactIR 1000 instrument. Therefore, the cyanide addition likely involves a monomeric Ti-based complex. A similar protocol was used to establish the overall rate expression and order for each of the reaction parameters. In these studies, substrate **5** and ligand **7** were employed (toluene, 18 °C), and *i*-PrOH was introduced at a constant rate. The order in **5** was established by determination of the kinetic rate constants at various concentrations of the substrate with 10 mol % Ti(O*i*-Pr)$_4$ and ligand **7**. A plot of ln[**5**]$_0$ versus ln *k* gave a straight horizontal line, indicating a zero-order dependence on the concentration of the substrate. When data were collected under the same conditions, but with varying amounts of TMSCN, a zero-order dependence on TMSCN was observed. Similar studies with *i*-PrOH indicated zero rate order. Catalytic additions carried out in the presence of TMSCN, *i*-PrOD, and **7** (pretreated with *i*-PrOD to ensure complete exchange of acidic protons) gave $k_H/k_D = 1.0 \pm 0.08$, suggesting that the turnover-limiting step of the catalytic cycle does not involve cleavage of a CH, NH, or an OH bond.

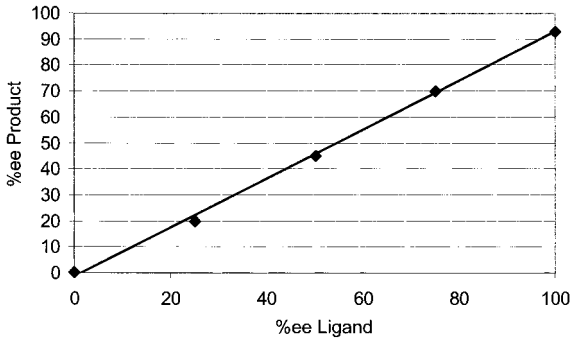

Figure 1. Plot of % ee product vs % ee ligand.

Various structural features of the chiral peptide ligand were systematically altered, and relative rates and enantioselectivities were measured. These studies, summarized in Scheme 2, led to several key observations. (1) Not only is the presence of the AA2 moiety critical to reactivity and enantioselectivity (compare **7** with **8**), its *stereochemical identity is of notable significance* (compare **7** with **9** and **10**). (2) The presence of a more Lewis basic amide carbonyl (vs a carboxylic ester) influences the rate of asymmetric cyanide addition. For instance, the initial rate of reaction (90 min) with ligand **7** is 2.3 times faster than that for the derived methyl ester **11**. The importance of the presence of AA2 and the significant influence of the related local chirality suggest that the peptide segment of the ligand might be *actively* participating in the asymmetric reaction, rather than simply providing steric differentiation that leads to absolute π-facial selectivity.

The proposed participation of the AA2 unit suggests that the turnover-limiting step involves a highly ordered transition state. Accordingly, activation parameters were measured for the asymmetric Ti-catalyzed cyanide addition to **5** through k_{obs} values measured at 5 °C intervals between −15 and +20 °C. Calculations from an Eyring plot (Figure 2) give $\Delta H^{\ddagger} = 8.98 \pm 1.3$ kcal mol^{-1} and $\Delta S^{\ddagger} = -45.6 \pm 4.1$ cal K^{-1} mol^{-1}.

The large and negative entropy of activation, together with the aforementioned data, are consistent with a rapid and reversible H-bond formation between HNC and AA2 carbonyl (cf., ester terminus less effective than AA2 amide)[15] and a turnover-limiting cyanide delivery to the Ti-bound substrate via the rigid transition structure in Figure 3.[16−18] Subsequent and

(12) An alternative pathway would involve direct participation of TMSCN (vs HCN), where the effect of added *i*-PrOH is not to generate HCN. Rather, the AA2 carbonyl may first react with TMSCN to form a zwitterionic cyanide complex such as **i**. After the addition of CN to the substrate, *i*-PrOH would react with the silylated amide to generate *i*-PrOTMS, releasing the catalytic active ligand. Such a pathway is unlikely, because treatment of 50 mol % of **7** (cf., Scheme 2) and Ti(O*i*-Pr)$_4$ (complex preformed by removal of *i*-PrOH in vacuo) with imine **5** and TMSCN leads to only ~10% conversion (4 °C, 18 h, toluene; no *i*-PrOH).

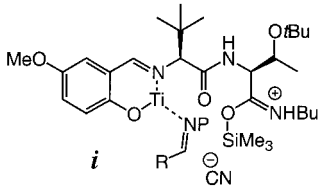

(13) For reviews of nonlinear effects in asymmetric catalysis, see: (a) Girard, C.; Kagan, H. B. *Angew. Chem., Int. Ed. Engl.* **1998**, *37*, 2922−2959. (b) Blackmond, D. G. *Acc. Chem. Res.* **2000**, *33*, 402−411.

(14) See the Supporting Information for all plots and details of kinetic measurements and spectroscopic studies.

Scheme 2

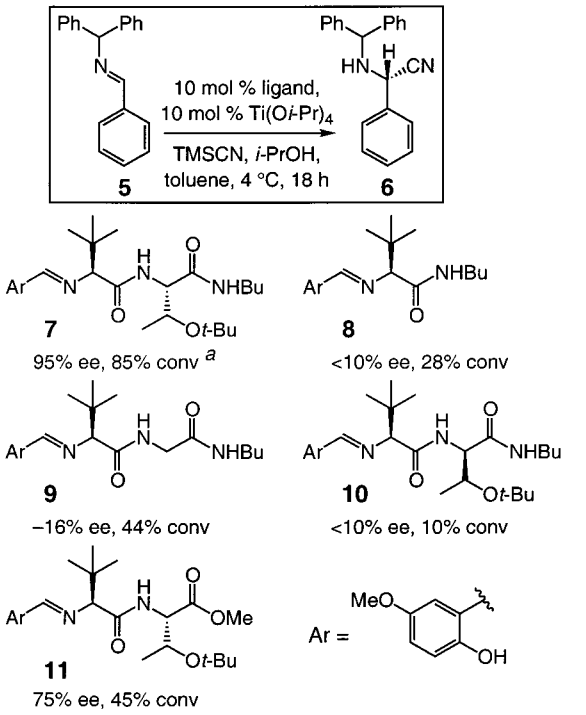

[a] Enantioselectivities measured by chiral HPLC (chiralpak AD); conversion measured by ^{1}H NMR.

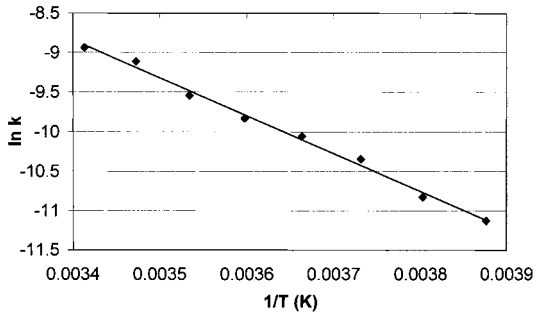

Figure 2. Eyring plot for Ti-catalyzed cyanide addition to imine **5**.

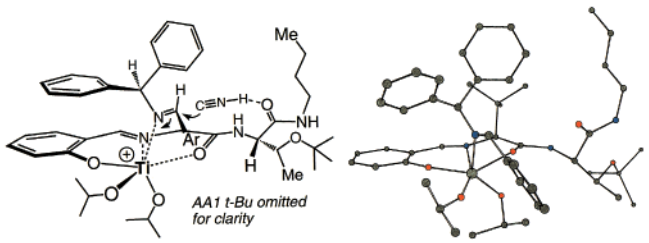

Figure 3.

facile loss of proton leads to the formation of the desired amino nitrile (cf., $k_H/k_D = 1.0 \pm 0.08$).[19]

Molecular modelings and calculations[20] involving imine **5** and peptidic Schiff base **7** suggest that, as shown in Figure 3, association of substrate to one face of the distorted octahedral Ti−Schiff base complex is energetically more favorable (top vs bottom face in Figure 3). More importantly, if metal−substrate association occurs from the alternative face of the Ti−peptide complex, the AA2 carbonyl cannot promote C−C bond formation readily, because the bulky AA2 substituent would be projected toward the catalyst structure during cyanide delivery (steric hindrance). The imine substrate, in its lower energy trans configuration, coordinates in a manner that minimizes steric interactions with the chiral Ti−peptide complex. It is in such a substrate−metal ensemble that the amide carbonyl of AA2 can readily reach and deliver HNC to the C=N bond to produce the major product enantiomer.

This proposal is consistent with the available kinetic and stereochemical data, including the importance of the stereochemical identity of the AA2 moiety (cf., Scheme 2). The model in Figure 3 provides a plausible rationale as to why the absence of such a substituent leads to diminution in reactivity and selectivity (compare **7** and **8** in Scheme 2). The stereochemistry of the AA2 moiety is critical to catalyst preorganization, rendering H-bonding between HNC and AA2 amide carbonyl and the formation of the C−C bond entropically more favorable. A Ti·peptide complex that bears an AA2 with the alternative stereochemistry is a less effective chiral catalyst (compare **7** and **10** in Scheme 2), as cyanide delivery would engender costly steric interactions involving the amino acid substituent and the O-*i*-Pr ligands of the transition metal. Finally, substrate coordination to the available equatorial site situates the imine in such a manner as to give rise to unfavorable steric repulsions between the phenyl moieties of the N-protecting group and the AA2 residue, which must remain within a proper distance to be able to deliver HNC.

Extensive spectroscopic studies of Ti·ligand complexes have been carried out. Treatment of ligand **2** with 1 equiv of Ti(O*i*-Pr)$_4$ at 22 °C leads to the formation of multiple species (400 MHz ^{1}H NMR; toluene-d_8); the resulting solution can be used to promote cyanide additions to imines efficiently and selectively. When the sample is heated to 100 °C, the spectrum simplifies significantly and remains so when it is cooled to 22 °C. ^{1}H NMR analysis indicates the presence of two complexes (9:1), the major component of which was analyzed by ^{1}H and ^{13}C NMR, gCOSY, and HETCOR spectral analyses,[13] suggesting that **12** is the major entity.[21] As the representative data in Scheme 3 indicate, significant downfield shifts in the ^{13}C NMR, especially of the two amide carbons, imply association of both the AA1 and AA2 sites to the transition metal center. Disap-

(15) Because a deuterium isotope effect is not detected, it follows that dissociation of N−H bond does not occur during the turnover-limiting step. These considerations indicate that H-bonding likely involves the N−H of HNC, not the C−H of HCN, because in the latter case, cleavage of a C−H bond would have to occur in the slowest step of the catalytic cycle (as the C−C bond is being formed).

(16) ^{13}C NMR spectroscopic studies involving TMS^{13}CN do not indicate the presence of a Ti−CN complex. Similar conclusions are reached after the results of IR studies are compared with reported literature values. See: Belokon, Y. N.; Green, B.; Ikonnikov, N. S.; Larichev, V. S.; Lokshin, B. V.; Moscalenko, M. A.; North, M.; Orizu, C.; Peregudov, A. S.; Timofeeva, G. I. *Eur. J. Org. Chem.* **2000**, 2655−2661.

(17) For a related mechanism involving a bimolecular delivery of HCN to aldehydes, see: Corey, E. J.; Wang, Z. *Tetrahedron Lett.* **1993**, *34*, 4001−4004.

(18) It is unlikely that the active complex is one where the AA2 carbonyl is bound to the Ti center (no internal delivery). If this were the case (simple cyanide addition to the bound imine), the value for entropy of activation would likely be significantly smaller, because a notably lesser degree of rigidity would take place within the transition structure. Moreover, in the absence of a base, it is unlikely that the AA2 carbonyl can displace an O-*i*-Pr ligand from the Ti center.

(19) Alternatively, it may be suggested that a rapid and reversible association of HCN with the AA2 amide bond precedes cyanide addition. This scenario is less favored on the basis of the substantial pK_a difference between HCN and a protiated amide (~9 and <0, respectively); see: *Handbook of Chemistry and Physics*, 73rd ed.; Lide, D. R., Ed.; CRC Press: Ann Arbor, MI, 1993.

(20) Calculations were carried out with Spartan SGI (version 5.1.1) at the semiempirical PM3 (tm) level. See the Supporting Information for details.

(21) For previous reports regarding the structure of related Ti complexes, see: (a) Hayashi, M.; Miyamoto, Y.; Inoue, T.; Oguni, N. *J. Org. Chem.* **1993**, *58*, 1515−1522. (b) Flores-Lopez, L. Z.; Parra-Hake, M.; Somanathan, R.; Walsh, P. J. *Organometallics* **2000**, *19*, 2153-2160 and references therein.

Scheme 3. Representative ^{1}H and ^{13}C NMR Data for the Unreactive Ti·L Complex (**12**)

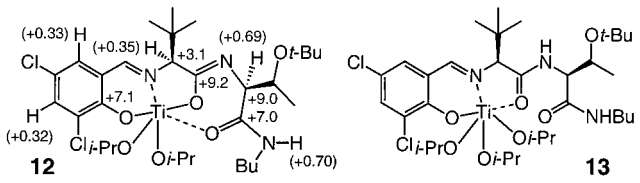

pearance of the AA1 amide NH and the significant downfield shifts in the ^{1}H NMR spectrum further support this proposal ($\Delta\delta$ in parentheses). However, we soon discovered that the complex generated upon heating, which is stable after cooling to 22 °C and exhibits the simpler NMR spectra, is *catalytically inactive*.

Several plausible explanations may be put forward for the inactivity of **12**. (1) According to molecular models, AA2 carbonyl association with the Ti center is geometrically more constrained than that of the AA1 unit. Furthermore, the covalently bound oxygen ligand of AA1 moiety in **12** is expected to be less electron donating than an O*i*-Pr. Thus, the relatively electron poor Ti in **12** would be less prone to convert to a catalytically active cationic Ti complex by loss of an alkoxide.[22] (2) The more rigidly constrained AA2 unit in **12** is expected to be less effective in delivering HNC to the coordinated substrate (see Figure 3). Previous considerations suggest that a complex such as **13** should be more active, because the derived cationic Ti would be more accessible. An O*i*-Pr ligand may more readily dissociate from a tri-isopropoxide Ti complex such as **13**, because the metal center is more electron rich by (i) the more accessible AA1 carbonyl as the coordinating Lewis base (vs AA2 carbonyl) and (ii) the additional stronger Lewis basic isopropoxide (vs AA1 amide oxygen).[23]

Conclusions

Findings disclosed herein demonstrate that, by the virtue of their structural and stereochemical identity, peptidic Schiff bases can serve as bifunctional catalysts to deliver appreciable reactivity and high enantioselectivity. It must be noted that, although the above mechanistic hypotheses offer a plausible and consistent rationale that accounts for numerous features of the asymmetric Ti-catalyzed cyanide additions, they fail to explain the more subtle attributes of this class of transformations. One such example involves variations in the Schiff base (SB) moiety of the optimal chiral ligand as a function of the identity of different substrates.[6] It is, after all, such subtle energetic modulations that often make it nearly impossible to predict, a priori, the exact identity of the most effective catalyst.[1] Nonetheless, the hypotheses presented herein are important, because they bear notable implications vis-á-vis mechanisms of other asymmetric processes promoted by this class of ligands. For instance, our initial studies indicate that, in a similar fashion as detailed previously, in the Zr-catalyzed alkylations of imines by dialkylzincs[5] and Cu-catalyzed conjugate additions of dialkylzincs to enones,[6] the presence and the stereochemical identity of the AA2 moiety is crucial to the reaction efficiencies and selectivities. Investigations toward establishing the generality of the principles presented here, and their application to the development of new catalytic asymmetric C−C bond forming reactions, are in progress.

(22) For a study on the effect of electron density on alkoxide ligand exchange in Ti complexes, see: Campbell, C.; Bott, S.; Larsen, R.; Van DerSluys, W. *Inorg. Chem.* **1994**, *33*, 4950−4958.

(23) It is less likely that dissociation of the AA2 carbonyl from **12** would yield an active Ti complex. This would lead to the formation of a coordinatively unsaturated, but neutral, Ti center, which may only weakly bind the imine substrate and not provide efficient activation towards cyanide addition. In a similar fashion, association of an O*i*-Pr instead of the AA1 carbonyl is possible but would yield a less Lewis acidic transition metal center.

Experimental Section

General. ReactIR spectra were recorded on an ASI Inc. ReactIR spectrophotometer, ν_{max} in cm^{-1}. ReactIR and QuantIR software are products of ASI Inc. Infrared (IR) spectra were recorded on a Perkin-Elmer 781 spectrophotometer, ν_{max} in cm^{-1}. Bands are characterized as broad (br), strong (s), medium (m), and weak (w). ^{1}H NMR spectra were recorded on a Varian Unity 300 (300 MHz) or Varian Gemini 2000 (400 MHz). Chemical shifts in ppm from tetramethylsilane are reported with the solvent resonance as the internal standard ($CHCl_3$, δ 7.26; $PhCH_3$, δ 2.34). Data are reported as follows: chemical shift, integration, multiplicity (s = singlet, d = doublet, t = triplet, q = quartet, br = broad, m = multiplet), coupling constants (Hz), and assignment. ^{13}C NMR spectra were recorded on a Varian Unity 300 (75 MHz) or Varian Gemini 2000 (100 MHz) with complete proton decoupling. Chemical shifts are reported in ppm with the solvent as the internal reference ($CDCl_3$, δ 77.0; $PhCH_3$, δ 21.0). Enantiomer ratios were determined by high-pressure liquid chromatography (HPLC) using a Shimadzu chromatograph and a chiralpak AD column (4.6 mm × 250 mm chiral column by Chiral Technologies).

All reactions were conducted in oven (135 °C) and flame-dried glassware under an inert atmosphere of dry argon or nitrogen. DMF (99.9%), diphenylmethyl amine, *tert*-leucine, and all commercially available aldehydes were purchased from Aldrich and used without further purification. Trimethylsilylcyanide and Ti(O*i*-Pr)$_4$ (99.99%) were purchased from Aldrich and distilled prior to use. All amino acids, 1-(3-dimethylaminopropyl)-3-ethyl-carbodiimide (EDC), *N*-hydroxybenzotriazole (HOBt), and piperidine were purchased from Advanced Chemtech and used without further purification. Toluene was distilled from sodium/benzophenone ketal. 2-Propanol was distilled from $CaSO_4$.

5-Methoxy-salicyl-*t*-Leu-Thr(*t*-Bu)-NHBu (7). Fmoc-Thr(*t*-Bu) (20 g, 50 mmol) was dissolved in 200 mL of CH_2Cl_2 and cooled to 0 °C. HOBT (7.7 g, 50 mmol), EDC (9.6 g, 50 mmol), and *n*-butyl amine (11 mL, 110 mmol) were added directly to the reaction mixture in succession. The solution was allowed to warm to 22 °C and stirred for 12 h. The reaction was quenched upon addition of 100 mL of a 10% citric acid solution, and the mixture was washed with 2 × 200 mL portions of citric acid and 2 × 100 mL portions of saturated aqueous $NaHCO_3$. The organic layer was washed with 1 × 100 mL of brine, dried over $MgSO_4$, filtered, and concentrated in vacuo to afford a white solid. This solid was dissolved in 100 mL of CH_2Cl_2, and piperidine (10 mL, 100 mmol) was added at 22 °C. After 2 h, the mixture was concentrated in vacuo and purified by silica gel chromatography (gradient from ethyl acetate to 4:1 ethyl acetate/MeOH) to afford H_2N-Thr(*t*-Bu)-Bu as a light orange oil. This oil was dissolved in 100 mL of CH_2Cl_2, HOBT (6.2 g, 40 mmol) and EDC (7.7 g, 40 mmol) were added, and the reaction was subsequently cooled to 0 °C. Fmoc-*t*-Leu (14 g, 40 mmol) and Et_3N (7.0 mL, 50 mmol) were introduced, and the resulting solution was stirred for 12 h at 22 °C. The reaction was quenched upon addition of 50 mL of a 10% citric acid solution. The organic layer was removed and subsequently washed with 1 × 100 mL of an aqueous 10% citric acid solution and 2 × 100 mL solutions of saturated aqueous $NaHCO_3$. The organic layer was washed with 1 × 50 mL of brine, dried over $MgSO_4$, filtered, and concentrated in vacuo to afford a white solid. The resulting solid was dissolved in 50 mL of CH_2Cl_2, and piperidine (8.0 mL, 81 mmol) was added at 22 °C. After 2 h, the mixture was concentrated in vacuo and purified by silica gel chromatography (gradient from ethyl acetate to 4:1 ethyl acetate/MeOH) to afford H_2N-*t*-Leu-Thr(*t*-Bu)-Bu as a white solid. The resulting solid was dissolved in 20 mL of CH_2Cl_2 and treated with 5-methoxysalicylaldehyde (3.5 mL, 28 mmol) and $MgSO_4$ (100 mg × 10 mmol) for 16 h at 22 °C. The solution was filtered and concentrated in vacuo to afford a yellow solid. Recrystallization from MeOH/H_2O (10:1) provided a yellow solid (8.3 g, 17 mmol, 35% yield). IR (neat, NaCl): 3322 (br), 2964 (s), 2927 (s), 2865 (m), 1664 (s), 1497 (s),

1356 (m), 1275 (s), 1084 (m), 1041 (m), 776 (m), 777 (m) cm^{-1}. ^1H NMR ($CDCl_3$, 400 MHz): 12.06 (1H, s, O**H**), 8.20 (1H, s, **H**C═N), 7.19 (1H, d, $J = 3.8$, aromatic **H**), 6.92−6.89 (3H, m, aromatic **H** and Thr N**H**), 6.74 (1H, s, aromatic **H**), 4.24−4.16 (2H, m, Thr-α**H** and Thr-β**H**), 3.74 (3**H**, s, OCH_3), 3.50 (1H, s, Tle-α**H**), 3.34−3.24 (1H, m, NHC**H**$_2$Pr), 3.18−3.08 (1H, m, NHC**H**$_2$Pr), 1.44−1.36 (2H, m, $NHCH_2C\mathbf{H}_2Et$), 1.33−1.19 (12H, m, Thr $C(C\mathbf{H}_3)_3$ and $NH(CH_2)_2C\mathbf{H}_2$-CH_3), 1.03 (9H, s, Tle $C(C\mathbf{H}_3)_3$), 0.85 (6H, apparent t, Thr β$C\mathbf{H}_3$ and $NH(CH_2)_3C\mathbf{H}_3$). ^{13}C NMR ($CDCl_3$, 100 MHz): 170.9, 169.7, 167.2, 156.0, 153.1, 121.2, 119.1, 118.9, 116.2, 85.2, 76.4, 67.1, 58.3, 37.0, 40.2, 36.2, 32.5, 29.4, 28.4, 21.2, 18.6, 14.9. HRMS (ES) calcd for $C_{26}H_{44}N_3O_5$ ($M + H^+$), 478.3281; found, 478.3284.

5-Methoxy-salicyl-*t*-Leu-(D)-Thr(*t*-Bu)-NHBu (10). IR (neat, NaCl): 3326 (br), 2961 (s), 1652 (s), 1589 (m), 1459 (s), 1362 (m), 1280 (s), 1086 (m), 1035 (m), 991 (m), 783 (m), 733 (m) cm^{-1}. ^1H NMR ($CDCl_3$, 400 MHz): δ 12.07 (1H, s), 8.21 (1H, s), 7.05 (1H, d, $J = 5.7$), 6.93−6.88 (2H, m), 6.75 (1H, d, $J = 2.4$), 4.30 (1H, dd, $J = 3.9, 5.7$), 4.07 (1H, dq, $J = 6.4, 3.8$), 3.73 (3H, s), 3.52 (1H, s), 3.55−3.28 (1H, m), 3.21−3.13 (1H, m), 1.48−1.41 (2H, m), 1.37−1.28 (2H, m), 1.20 (9H, s), 1.02 (9H, s), 0.89−0.84 (6H, m). ^{13}C NMR ($CDCl_3$, 100 MHz): δ 170.3, 169.0, 166.1, 155.3, 152.3, 120.3, 118.2, 118.1, 115.3, 84.3, 75.5, 66.1, 57.2, 56.1, 39.3, 35.2, 31.6, 28.3, 27.3, 20.2, 17.3, 13.8. HRMS (ES) calcd for $C_{26}H_{44}N_3O_5$ ($M + H^+$), 478.3281; found, 478.3272.

5-Methoxy-salicyl-*t*-Leu-Gly-NHBu (9). IR (neat, NaCl): 3307 (br), 2955 (s), 2867 (m), 1652 (s), 1488 (s), 1274 (m), 1161 (m), 1035 (m) cm^{-1}. ^1H NMR ($CDCl_3$, 400 MHz): δ 12.02 (1H, s), 8.21 (1H, s), 6.93 (1H, d, $J = 2.9$), 6.90 (1H, s), 6.77−6.61 (1H, m), 6.75 (1H, d, $J = 2.7$), 6.34−6.27 (1H, m), 3.94 (1H, dd, $J = 5.6, 16.1$), 3.80 (1H, dd, $J = 5.6, 16.1$ Gly αH), 3.77 (3H, s), 3.55 (1H, s), 3.22−3.17 (2H, m), 1.45−1.22 (4H, m), 1.02 (9H, s), 0.85 (3H, apparent t, 7.1). ^{13}C NMR ($CDCl_3$, 100 MHz): δ 171.2, 168.7, 166.8, 155.1, 152.5, 120.6, 118.2, 115.5, 83.8, 56.1, 43.4, 39.5, 35.4, 31.7, 27.3, 20.2. HRMS (ES) calcd for $C_{20}H_{32}N_3O_4$ ($M + H^+$), 378.2393; found, 378.2380.

5-Methoxy-salicyl-*t*-Leu-Thr(*t*-Bu)-OMe (11). IR (neat, NaCl): 3417 (br), 2971 (s), 1749 (s), 1674 (s), 1495 (s), 1273 (s), 1204 (m), 1078 (m), 777 (w) cm^{-1}. ^1H NMR ($CDCl_3$, 400 MHz): δ 12.17 (1H, s), 8.27 (1H, s), 6.92 (1H, d, $J = 2.7$), 6.89 (1H, s), 6.79 (1H, d, $J = 2.8$), 6.68 (1H, d, $J = 8.8$), 4.38 (1H, dd, $J = 9.0, 1.6$) 4.18 (1H, dq, $J = 6.4, 1.8$), 3.75 (3H, s), 3.59, (3H, s), 3.54 (1H, s), 1.19 (3H, d, $J = 6.2$), 1.05 (9H, s), 1.02 (9H, s). ^{13}C NMR ($CDCl_3$, 100 MHz): δ 171.2, 170.9, 166.7, 155.3, 152.4, 120.4, 118.3, 118.0, 115.4, 83.8, 74.2, 67.2, 58.0, 56.1, 52.35, 35.1, 28.4, 27.3, 21.8. HRMS (ES) calcd for $C_{19}H_{29}N_2O_6$ ($M + H^+ - C(CH_3)_3$), 381.2026; found, 381.2038.

5-Methoxy-salicyl-*t*-Leu-NHBu (8). IR (neat, NaCl): 3310 (br), 2959 (s), 2865 (m), 1649 (s), 1492 (s), 1273 (s), 1160 (m), 1028 (m), 777.8 (w) cm^{-1}. ^1H NMR ($CDCl_3$, 400 MHz): δ 12.18 (1H, s), 8.21 (1H, s), 6.94 (1H, d, $J = 2.9$), 6.90 (1H, s), 6.77 (1H, d, $J = 2.9$), 5.91−5.84 (1H, m), 3.75 (3H, s), 3.52 (1H, s), 3.37−3.28 (1H, m), 3.15−3.07 (1H, m), 1.48−1.40 (1H, m), 1.33−1.25 (2H, m), 1.01 (9H, s), 0.86 (3H, t, $J = 7.3$). ^{13}C NMR ($CDCl_3$, 100 MHz): δ 170.0, 166.5, 154.9, 152.6, 120.5, 118.2, 117.9, 115.4, 84.0, 56.1, 39.2, 35.1, 31.8, 27.3, 20.3, 13.9. HRMS (ES) calcd for $C_{18}H_{29}N_2O_3$ ($M + H^+$), 321.2178; found, 321.2172.

Procedure for synthesis of benzaldimine **5**: Benzaldehyde (50 mmol, 5.0 mL), diphenylmethylamine (50 mmol, 8.6 mL), and $MgSO_4$ (1.0 g) in benzene (100 mL) were stirred for 8 h at 22 °C. The solution was filtered and concentrated in vacuo. The product was purified by recrystallization (Et_2O, hexanes) to provide a white solid (12.6 g, 46 mmol, 93% yield).

Benzaldehyde Diphenylmethyl Imine (5). IR (CCl_4, NaCl): 3081 (w), 3062 (w), 3037 (w), 2842 (w), 1646 (m), 1495 (m), 1457 (m), 746 (m), 690 (s) cm^{-1}. ^1H NMR ($CDCl_3$, 400 MHz): δ 8.40 (1H, d, $J = 2.4$), 7.84−7.81 (2H, m), 7.41−7.20 (13H, m), 5.58 (1H, d, $J = 2.4$). ^{13}C NMR ($CDCl_3$, 100 MHz): δ 161.4, 144.5, 137.0, 131.4, 129.2, 129.1, 129.1, 128.3, 127.6, 78.6. HRMS (ES) calcd for $C_{20}H_{17}N$, 271.1361; found, 271.1354. Anal. Calcd for $C_{20}H_{17}N$: C, 88.52; H, 6.31; N, 5.16. Found: C, 88.59; H, 6.34; N, 5.04.

Procedure for Ti-Catalyzed Cyanide Addition to Imines. In a glovebox, chiral ligand (0.010 mmol) was placed into a flame-dried round-bottomed flask and was dissolved in toluene (0.50 mL). The flask was charged with Ti(O*i*-Pr)$_4$ (60 μL of a 0.10 M solution in toluene, 0.010 mmol), and the resulting yellow solution was stirred for 10 min at 22 °C. Subsequently, the imine (0.10 mmol) was added as a solid. The reaction vessel was capped with a septum, sealed with Teflon tape, and transferred from the glovebox to a room maintained at 4 °C. The flask was equipped with a balloon of argon, and TMSCN (27 μL, 0.20 mmol) was added by syringe to the stirred solution. *i*-PrOH (15 μL, 0.20 mmol) in toluene (1.0 mL) was added dropwise by a syringe pump over 20 h (50 μL/h), with additional stirring for another 4 h. Reaction was quenched through addition of wet Et_2O (5 mL) and passed through a plug of silica gel with 3 mL of CH_2Cl_2. Purification by silica gel chromatography and conversion and enantioselectivity levels were determined by chiral HPLC analysis (chiralpak AD, 90:10 EtOAc/hexanes, 1 mL/min, 254 nm).

Diphenylmethylaminophenylacetonitrile (6). The general procedure was followed with 5-methoxy-salicyl-*t*-Leu-Thr(*t*-Bu)-NHBu (**7**) (49 mg, 0.10 mmol), Ti(O*i*-Pr)$_4$ (0.10 mmol, 0.20 mL of a 0.50 M solution in toluene), benzaldehyde diphenylmethyl imine (**5**) (270 mg, 1.0 mmol), and TMSCN (270 μL, 2.0 mmol) in toluene (2.5 mL). *i*-PrOH (150 μL, 2.0 mmol) in toluene (2.0 mL) was added over 20 h with additional stirring for 10 h. The unpurified reaction mixture was passed through a plug of silica with CH_2Cl_2 (5.0 mL), and volatiles were removed in vacuo. The resulting pale yellow solid was recrystallized from 5:1 hexanes/CH_2Cl_2 to afford 230 mg of **6** as a white solid (82% yield, >99% ee). (The unpurified reaction mixture gave 99% conversion and 97% ee by HPLC.) IR (CCl_4, NaCl): 3327 (m), 3087 (s), 3069 (s), 3031 (s), 2848 (m), 2231 (w), 1948 (m), 1879 (m), 1810 (m), 1608 (m), 1501 (s), 1451 (s), 1187 (m), 929 (m) cm^{-1}. ^1H NMR ($CDCl_3$, 400 MHz): δ 7.58−7.20 (15H, m), 5.24 (1H, s), 4.59 (1H, d, $J = 12.0$), 2.14 (1H, d, $J = 12.0$). ^{13}C NMR ($CDCl_3$, 100 MHz): δ 143.4, 141.7, 135.6, 129.7, 129.6, 129.4, 128.6, 128.4, 128.1, 127.9, 127.7, 119.4, 66.2, 53.0. HRMS (ES) calcd for $C_{21}H_{18}N_2$ ($M + H^+$), 299.1548; found, 299.1549. Anal. Calcd for $C_{21}H_{18}N_2$: C, 84.53; H, 6.08; N, 9.39. Found: C, 84.22; H, 6.19; N, 9.28. $[\alpha]^{24}_D$ −64.2 ± 0.1° (*c* 5.0, $CHCl_3$).

Study of Nonlinear Effects. In a glovebox, 98 μL (0.010 mmol) of a Ti(O*i*-Pr)$_4$ solution (60 μL Ti(O*i*-Pr)$_4$ in 2.0 mL of toluene) was added to 200 μL (0.010 mmol) of a 0.05 M solution of (L)-Ligand **7** (72 mg in 2.6 g of toluene) and allowed to stir at 22 °C for 5 min. Imine **5** (27 mg, 0.10 mmol) was added, followed by 300 μL of toluene. The flask was sealed with a septum and moved from the glovebox to a cold room maintained at 4 °C. The flask was equipped with a syringe containing 1 mL of a solution of *i*-PrOH (15 μL in 1.0 mL toluene) affixed to a digital (electronically controlled) syringe pump (50 μL/h addition rate). The reaction vessel was allowed to equilibrate to +4 °C for 5 min with stirring, at which time 22 μL (0.20 mmol) of TMSCN was added through syringe and the addition of *i*-PrOH was initiated by the syringe pump. After 18 h, the reaction was quenched with wet ether and concentrated in vacuo. The yellow solid was dissolved in ethyl acetate and passed through a plug of silica gel with 3 mL of CH_2Cl_2. The resulting solution was concentrated in vacuo and analyzed by ^1H NMR spectroscopy and chiral HPLC (see general procedure above), indicating the formation of the desired amino nitrile in 93% ee (normalized (set to 1) for plotting purposes). Additional data, as illustrated in Figure 2, were collected in a similar fashion.

Measurement of Initial Rate Difference between Reactions of 5-Methoxy-salicyl-*t*-Leu-Thr(*t*-Bu)-Bu (7) and 5-Methoxy-salicyl-*t*-Leu-Thr(*t*-Bu)-OMe (11). In a glovebox, an oven-dried ReactIR flask was charged with 200 μL (0.010 mmol) of a 0.05 M solution of ligand **7** (0.12 g in 5.0 mL toluene), 400 μL (0.10 mmol) of a 0.25 M solution of imine **5** (1.0 g in 15 mL of toluene), and 200 μL (0.010 mmol) of a 0.05 M solution Ti(O*i*-Pr)$_4$ (74 μL of Ti(O*i*-Pr)$_4$ in 5.0 mL of toluene). Upon addition of Ti(O*i*-Pr)$_4$, the solution turned from yellow to bright orange. The flask was removed from the glovebox, and the IR probe was submerged into the reaction mixture. A 1 mL syringe containing a solution of *i*-PrOH (18 μL, 0.24 mmol in 1 mL of toluene), connected to an electronically controlled syringe pump (50 μL/h addition rate), was attached to the reaction flask. ReactIR data collection was initiated immediately after TMSCN (22 μL, 0.20 mmol) was added to the reaction mixture and addition of the *i*-PrOH solution was started through a syringe pump. IR spectra were collected at 1 min intervals for 2 h

and were imported into the QuantIR software where the spectra were analyzed applying the calibration curve (see the Supporting Information).

Eyring Plot Measurements. In a glovebox, an oven-dried ReactIR flask was charged with 100 μL (0.012 mmol) of a 0.12 M solution of ligand **7** (400 mg in 8.1 g toluene), 100 μL (0.12 mmol) of a 1.2 M solution of imine **5** (5.0 g in 18 g of toluene), 24 μL (0.012 mmol) of a 0.50 M solution of Ti(O*i*-Pr)$_4$ (30 μL of Ti(O*i*-Pr)$_4$ in 2.0 mL of toluene), and 280 μL of toluene. Upon addition of Ti(O*i*-Pr)$_4$, the solution turned from yellow to bright orange. The flask was removed from the glovebox, and the IR probe was immersed into the mixture which is then submerged into an ethylene glycol bath maintained at −15 °C by a circulation bath. A 1 mL volume of a solution of *i*-PrOH (18 μL, 0.24 mmol in 1.0 mL of toluene) was placed in a syringe connected to an electronically controlled syringe pump (50 μL/h addition rate) attached to the flask. TMSCN (22 μL, 0.20 mmol) was added, and *i*-PrOH (electronically controlled addition) addition was initiated. IR spectra were collected at 1 min intervals for 2−4 h and imported into the QuantIR software where the spectra were analyzed applying the calibration curve (see the Supporting Information).

Representative Measurement of Reaction Rate. (See the Supporting Information for full and further details.) In a glovebox, an oven-dried ReactIR flask was charged with 250 μL (0.030 mmol) of a 0.12 M solution of ligand **7** (400 mg in 8.1 g of toluene), 250 μL (0.30 mmol) of a 1.2 M solution of imine **5** (5.0 g in 18 g of toluene), and 30 μL (0.030 mmol) of a 1.0 M solution of Ti(O*i*-Pr)$_4$ (60 μL of Ti(O*i*-Pr)$_4$ in 2 mL of toluene). Upon addition of Ti(O*i*-Pr)$_4$, the solution turned from pale yellow to bright orange. The reaction flask was removed from the glovebox, and the IR probe was submerged into the reaction mixture. A 1 mL volume of a solution of *i*-PrOH (46 μL, 0.60 mmol in 1 mL of toluene) was placed in a syringe connected to an electronically controlled syringe pump (50 μL/h addition rate) which was in turn attached to the reaction vessel. ReactIR data collection was initiated immediately after TMSCN (75 μL, 0.60 mmol) was added to the reaction mixture and addition of the *i*-PrOH solution was started through a syringe pump. IR spectra were collected at 1 min intervals for 2 h and imported into the QuantIR software where the spectra were analyzed by applying the calibration curve (see the Supporting Information).

Measurement of Kinetic Isotope Effects. Chiral ligand **7** (25 mg, 0.05 mmol) was dissolved in *i*-PrOD and allowed to stir under an atmosphere of Ar for 2 days. At this time, the solution was concentrated in vacuo. Analysis of ^{1}H NMR of the recovered ligand indicated complete (>98%) disappearance of amide and phenol proton signals. A ReactIR vessel was charged with 4.8 mg (0.010 mmol) of deuterated **7**, 27 mg (0.10 mmol) of imine **5**, 500 μL of toluene, and 98 μL (0.010 mmol) of a 0.10 M solution of Ti(O*i*-Pr)$_4$ in toluene. Upon addition of Ti(O*i*-Pr)$_4$, the solution turned from yellow to bright orange in color. The flask was removed from the glovebox, and the IR probe was submerged into the mixture. A 1 mL syringe containing a solution of *i*-PrOD (15 μL, 0.20 mmol in 1 mL of toluene), connected to an electronically controlled syringe pump (50 μL/h addition rate), was attached to the flask. Data collection was carried out in the manner described previously.

Acknowledgment. This research was supported by the National Institutes of Health (GM-57212). We thank Professors D. L. McFadden (Boston College), L. T. Scott (Boston College), W. von E. Doering (Harvard), and C. L. Perrin (University of California, San Diego) and Mr. James R. Porter (Boston College) for helpful discussions.

Supporting Information Available: Detailed data on various measurements (19 pages, PDF). This material is available free of charge via the Internet at http://pubs.acs.org.

JA011875W